Far-Infrared Studies of Spin-Peierls Materials in a Magnetic Field

G. Li, J. S. Lee, V. C. Long, and J. L. Musfeldt*

Department of Chemistry, State University of New York at Binghamton, Binghamton, New York 13902-6016

Y. J. Wang

National High Magnetic Field Laboratory, Florida State University, Tallahassee, Florida 32306

M. Almeida

Departamento de Química, Instituto Tecnológico e Nuclear, P-2686 Sacavem Codex, Portugal

A. Revcolevschi and G. Dhalenne

Laboratoire de Chimie des Solides Université Paris-Sud, 91405 Orsay Cédex, France

We report the low-temperature far-infrared response of two prototypical spin-Peierls (SP) materials as a function of magnetic field in order to characterize the microscopic nature of the SP and high-field incommensurate phases. For the linear chain inorganic compound, $GeCuO_3$, we observe that the B_{3u} shearing mode is sensitive to the high-field phase boundary in the $H-T$ phase diagram, and we find Zeeman splitting of the zone–center spin-Peierls gap within the dimerized phase. In contrast, for the organic molecular conductor MEM-$(TCNQ)_2$, neither the electron–phonon coupling modes nor the low-energy lattice modes were found to be sensitive to the high-field phase boundary. We attribute this difference to the extended vs molecular structure of the two solids as well as to the extent of spin localization.

1. Introduction

Magnetic interactions in low-dimensional organic and inorganic solids have attracted a great deal of sustained interest over the past several decades.[1-6] For instance, considerable experimental and theoretical work has been undertaken to explore the competition between magnetism and superconductivity as well as the unique ordering properties of magnetic ground states. At the same time, synthesis of new materials has opened new opportunities to probe the physical characteristics of magnetic solids and underscored the long-range potential of tuning magnetic properties at a molecular level. However, the complexity of the chemical structure/physical property relationships has made the rational development of novel magnetic materials quite challenging.

The linear chain inorganic material $GeCuO_3$ is now attracting considerable interest as a model system for understanding magnetically driven phase transitions and the spin-Peierls (SP) ground state.[7-21] Other materials which display the elusive SP ground

(1) Grüner, G. *Rev. Mod. Phys.* **1994,** *66,* 1.
(2) Bray, J. W.; Interrante, L. V.; Jacobs, I. S.; Bonner J. C. In *Extended Linear Chain Compounds*; Miller, J. S., Ed.; Plenum: New York, 1983; Vol. 3.
(3) Inagaki, S.; Fukuyama, H. *Magnetic Properties of Low Dimensional Systems*; Falicov, L. M., Morán-Lópaz, J. L., Eds.; Springer-Verlag: New York, 1986.
(4) Ishiguro, T.; Yamaji, K. *Organic Superconductors*, Springer Series in Solid-State Sciences, Vol. 88; Springer-Verlag: Berlin, 1990.
(5) *Organic Conductors*; Farges, J. P., Ed.; Marcel-Dekker: New York, 1994.
(6) Kahn, O. *Molecular Magnetism*; VCH Publishers: New York, 1993.

(7) Hase, M.; Terasaki, I.; Uchinokura, K. *Phys. Rev. Lett.* **1994,** *70,* 3651.
(8) Hase, M.; Terasaki, I.; Uchinokura, K.; Tokunaga, M.; Miura, N.; Obara, H. *Phys. Rev. B* **1994,** *48,* 9616.
(9) Poirier, M.; Castonguay, M.; Revcolevschi, A.; Dhalenne, G. *Phys. Rev. B* **1995,** *52,* R6971.
(10) Nishi, M.; Fujita, O.; Akimitsu, A. *Phys. Rev. B* **1994,** *50,* 6508.
(11) Brill, T. M.; Boucher, J. P.; Voiron, J.; Dhalenne, G.; Revcolevschi, A.; Renard, J. P. *Phys. Rev. Lett.* **1994,** *73,* 1545.
(12) Fujita, O.; Akimitsu, J.; Nishi, M.; Kakurai, K. *Phys. Rev. Lett.* **1995,** *74,* 1677.
(13) Pouget, J. P.; Regnault, L. P.; Ain, M.; Hennion, B.; Renard, J. P.; Veillet, P.; Dhalenne, G.; Revcolevschi, A. *Phys. Rev. Lett.* **1994,** *72,* 4037.
(14) Lorenzo, J. E.; Hirota, K.; Shirane, G.; Tranquada, J. M.; Hase, M.; Uchinokura, K.; Kojima, H.; Tanaka, I.; Shibuya, Y. *Phys. Rev. B* **1994,** *50,* 1278.
(15) Mattheiss, L. F. *Phys. Rev. B* **1994,** *49,* 14050.
(16) Liu, X.; Wosnitza, J.; H. v. Löhneysen, Kremer, R. K. *Phys. Rev. Lett.* **1995,** *75,* 771.
(17) Y.-K. Kuo, Figueroa, E.; Brill, J. W. *Solid State Commun.* **1995,** *94,* 385.
(18) Dević, S. D.; Konstantinović, M. J.; Popović, Z.; Dhalenne, G.; Revcolevschi, A. *J. Phys. C.: Condens. Matter* **1994,** *6,* L745.
(19) Popović, Z. V.; Dević, S. D.; Popov, V. N.; Dhalenne, G.; Revcolevschi, A. *Phys. Rev. B* **1995,** *52,* 4185.
(20) Li, G.; Musfeldt, J. L.; Wang, Y. J.; Jandl, S.; Poirier, M.; Revcolevschi, A.; Dhalenne, G. *Phys. Rev. B* **1996,** *54,* R15633.
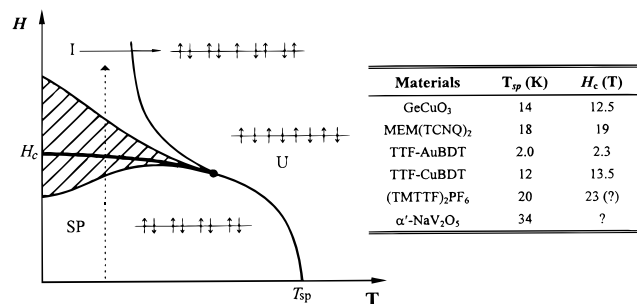(21) Bassi, M.; Camagni, P.; Rolli, R.; Samoggia, G. *Phys. Rev. B* **1996,** *54,* R11030.

Materials	T_{sp} (K)	H_c (T)
GeCuO$_3$	14	12.5
MEM(TCNQ)$_2$	18	19
TTF-AuBDT	2.0	2.3
TTF-CuBDT	12	13.5
(TMTTF)$_2$PF$_6$	20	23 (?)
α'-NaV$_2$O$_5$	34	?

Figure 1. The universal H-T phase diagram and critical temperatures/critical field values for several members of the family of SP materials. The arrow indicates the field-sweep path of our experiments.

state include several traditional molecular solids such as MEM(TCNQ)$_2$,TTF-CuBDT, TTF-AuBDT, and (TMTTF)$_2$PF$_6$, as well as the more recently discovered α'-NaV$_2$O$_5$ system.[2,22–35] These materials have substantial differences in structure and spin character. For instance, GeCuO$_3$ and α'-NaV$_2$O$_5$ display the extended linear chain structure of distorted octahedra and tetrahedra so often found in the oxides, whereas the other aforementioned materials are molecular in nature, held together only by van der Waals forces. The nature of the spin system is also important, as spins are highly localized in the inorganic material (d-type spins), whereas they are much more diffuse (and of π-origin) in the organic molecular conductors such as MEM(TCNQ)$_2$ or (TMTTF)$_2$ PF$_6$. The TTF-CuBDT and TTF-AuBDT materials provide for the possibility of π–d coupling as the Cu (or Au) is at the center of an organic π-system. The perylenes are another set of materials where complex structure and π–d coupling are important.[36,37]

Taken together, these compounds provide an excellent opportunity to study chemical structure/physical property relationships in magnetic solids. The universal magnetic field/temperature (H–T) phase diagram, characteristic of SP materials,[2] is shown in Figure 1 along with the spin-Peierls transition temperatures (T_{sp}) and critical field values (H_c) for several of the aforemen-

tioned materials. The structure of this diagram is at the heart of the ongoing work on both inorganic and organic SP compounds. In the inorganic prototype GeCuO$_3$, the high-temperature phase displays a uniform chain arrangement and a finite magnetic susceptibility, and the SP phase is dimerized and nonmagnetic due to the opening of a gap in the magnetic excitation spectrum.[7,11,12] Indeed, recent electron spin resonance, infrared, and neutron scattering experiments have provided a consistent picture of a system with two triplet-state gaps, at different places in the Brillouin zone.[10–12,20] The SP transition temperature is 14 K for GeCuO$_3$ at zero field, decreasing with applied magnetic field. In the organic prototype MEM(TCNQ)$_2$, the high-temperature phase displays a dimerized arrangement of the molecular building blocks and a tetramerized structure below the 18 K SP transition temperature.[29,30] (However, it is important to note that due to the 1:2 stoichiometry in the MEM(TCNQ)$_2$ charge-transfer salt, the spin structure is actually uniform above T_{sp} and dimerized below T_{sp}.) In each case, the second-order SP phase boundary is well described by the theory of Cross, with the coupling of the 3-D phonons and the 1-D spin system providing the underlying driving force for the transition.[2,3,38,39] In the MEM(TCNQ)$_2$ compound, the 8.5 cm^{-1} soft mode also plays an important role in the phase transition.[31] If the magnetic field is increased at low temperature, one passes from the nonmagnetic SP phase into a high-field magnetic phase. That the Zeeman energy dominates the spin–lattice energy above the critical field is the driving force for this transition.[2,3,22,38–42] The critical field, H_c, is 12.5 T for GeCuO$_3$.[7,8] Although less is known about the detailed nature of the high-field phase, structural studies and theoretical work point toward an incommensurate (I) soliton structure as the origin for the unusual properties.[2,3,22,38–42] Such a spin structure is diagrammed in Figure 1 and consists of a "spin kink" between two degenerate phases. This spin kink is actually delocalized over several lattice spacings,[2,22] and the incommensurate lattice modulation within the high-field exotic phase is field-dependent. Thus, raising the applied field in the I phase increases the concentration of spin solitons along the chain. The situation in the model organic SP system is quite similar, moving to the exotic high-field phase at about H_c = 19.5 T in MEM-(TCNQ)$_2$.[26,27] It is notable that MEM(TCNQ)$_2$ has a large hysteresis regime, indicative of the strongly first-order nature of this transition.

In order to provide further information on the lattice dynamics of the SP and magnetic phases, we have investigated the far-infrared response of both GeCuO$_3$ and MEM(TCNQ)$_2$ as a function of temperature and applied magnetic field. Here, we concentrate on the field-dependent results. Our overall goal is to obtain a microscopic characterization of each phase and to track the modes which are sensitive to the magnetoelastic transitions. That both molecular solids (such as MEM-(TCNQ)$_2$, TTF-CuBDT, and (TMTTF)$_2$ PF$_6$) and linear

(22) Bonner, J. C.; Northby, J. A.; Jacobs, I. S.; Interrante, L. V. *Phys. Rev. B.* **1987**, *35*, 1791.
(23) Erkelens, W. A. C.; Regnault, L. P.; Laugier, J.; Rossat-Mignod, J.; de Jongh, L. J. *Solid State Commun.* **1985**, *55*, 209.
(24) Harada, I.; Kotani, A. *J. Phys. Soc. Jpn.* **1982**, *51*, 1737.
(25) Huizinga, S.; Kommandeur, J.; Sawatzky, G. A.; Thole, B. T.; Kopinga, K.; de Jonge, W. J. M.; Roos, J. *Phys. Rev. B.* **1979**, *19*, 4723.
(26) Bloch, D.; Voiron, J.; Bonner, J. C.; Bray, J. W.; Jacobs, I. S.; Interrante, L. V. *Phys. Rev. Lett.* **1980**, *44*, 294.
(27) Bloch, D.; Voiron, J.; Bray, J. W.; Jacobs, I. S.; Bonner, J. C.; Kommandeur, J. *Phys. Lett.* **1981**, *82A*, 21.
(28) Northby, J. A.; Groenendijk, H. A.; de Jongh, L. J.; Bonner, J. C.; Jacobs, I. S.; Interrante, L. V. *Phys. Rev. B.* **1982**, *25*, 3215.
(29) Visser, R. J. J.; Oostra, S.; Vettier, C.; Voiron, J. *Phys. Rev. B.* **1983**, *28*, 2074.
(30) van Bodegom, B.; Larson, B. C.; Mook, H. A. *Phys. Rev. B.* **1981**, *24*, 1520.
(31) Tanaka, Y.; Satoh, N.; Nagasaka, K. *J. Phys. Soc. Jpn.* **1990**, *59*, 319.
(32) Blundell, S. J.; Pratt, F. L.; Pattenden, P. A.; Kurmoo, M.; Chow, K. H.; Takagi, S.; Jeständt, Th.; Hayes, W. *J. Phys.: Cond. Matter* **1997**, *9*, L119.
(33) Pouget, J. P.; *Mol. Cryst. Liq. Cryst.* **1982**, *79*, 129.
(34) Wzietec, P. *J. Phys. I.* **1993**, *3*, 171.
(35) Weiden, M.; Hauptmann, R.; Geibel, C.; Steglich, F.; Fischer, M.; Lemmens, P.; G. Güntherodt, *Z. Phys. B* **1997**, *103*, 1.
(36) Matos, M.; Bonfait, G.; Henriques, R. T.; Almeida, M. *Phys. Rev. B.* **1996**, *54*, 15307.
(37) Bonfait, G.; Matos, M. J.; Henriques, R. T.; Almeida, M. *Phys. B: Cond. Matter* **1995**, *211*, 297.

(38) Cross, M. C. *Phys. Rev. B.* **1979**, *20*, 4606.
(39) Cross, M. C.; Fischer, D. S. *Phys. Rev. B.* **1979**, *19*, 402.
(40) Kiryukhin, V.; Keimer, B.; Moncton, D. E. *Phys. Rev. Lett.* **1995**, *74*, 1669.
(41) Kiryukhin, V.; Keimer, B. *Phys. Rev. B.* **1995**, *52*, R704.
(42) Nakano, T.; Fukuyama, H. *J. Phys. Soc. Jpn.* **1980**, *49*, 1679.

chain inorganic magnetic materials (such as $GeCuO_3$, doped $GeCuO_3$ compounds, and α'-NaV_2O_5) display characteristic phases in $H-T$ space despite differences in spin localization, spin−orbit coupling, and structure is quite interesting. The purpose of this work is to explore the microscopic details of this unusual similarity.

2. Experimental Section

A large, regularly shaped single crystal of $GeCuO_3$ was grown by floating zone techniques using an image furnace.[43] The sample used for these experiments was cleaved from the original along the *bc*-plane and had dimensions of $\approx 0.5 \times 0.3 \times 0.15$ cm³. Large single crystals of $MEM(TCNQ)_2$ were grown by slow cooling of acetonitrile solutions as previously described for other complex TCNQ salts.[44,45] Typical sample dimensions were $\approx 0.4 \times 0.15 \times 0.05$ cm³. The $MEM(TCNQ)_2$ crystals were ground with paraffin at 77 K to prepare a sample suitable for transmission studies. This procedure was necessitated by the magnet setup, as detailed below. Infrared reflectance and transmission measurements were performed both at Binghamton and at the National High Magnetic Field Laboratory in Tallahassee, FL, using a Bruker 113V Fourier transform infrared spectrometer. Our runs were made using the 3.5, 12, 23, and 50 μm Mylar beam splitters, covering the frequency range from 25−600 cm⁻¹.

Both a 20 T superconducting magnet and a 33 T resistive magnet were employed for the magnetic field work.[46] It is important to mention that the higher field (resistive) magnet was needed for the $MEM(TCNQ)_2$ runs, as this sample has a critical field of 19.5 T. However, only transmission measurements are possible in this setup due to the very small (32 mm) bore size of the resistive magnet. A detailed description of the experimental setup at the National High Magnetic Field Laboratory is given elsewhere.[47] These measurements were performed using both the infrared reflectance probe (for the $GeCuO_3$) and the transmission probe (for the $MEM(TCNQ)_2$).[46] In the reflectance configuration, both the power reflectance and the relative reflectance are accessible. For instance, in a field we measure both the power reflectance through the phase transition as well as the reflectance ratio relevant to the field conditions $\Delta R = R(H)/R(0\ T)$. In contrast, the transmission probe limits us to a knowledge of the transmission ratio, $\Delta T = T(H)/T(0\ T)$, since we are only measuring single-beam spectra. Absolute transmission data was obtained separately.

Currently, it is not possible to probe polarization dependence in either probe geometry. However, polarization information, obtained from more standard experiments on single-crystal samples of $GeCuO_3$ and $MEM(TCNQ)_2$, is well-known. Since the overlap of vibrational structures is fairly minimal in each case, little information is lost due to the unpolarized nature of our measurements. Typical noise variations of the ratio files for different beam splitters in a magnetic field are on the order of 2−3%. Using both temperature and applied field, we are able to move around the $H-T$ phase diagram, taking spectra within each phase. In this way, we collected data which allows us to calculate all meaningful reflectance and transmission ratios for each sample. Here, we concentrate on the field dependence experiments, following the indicated path (SP → I) in Figure 1.

3. Results and Discussion

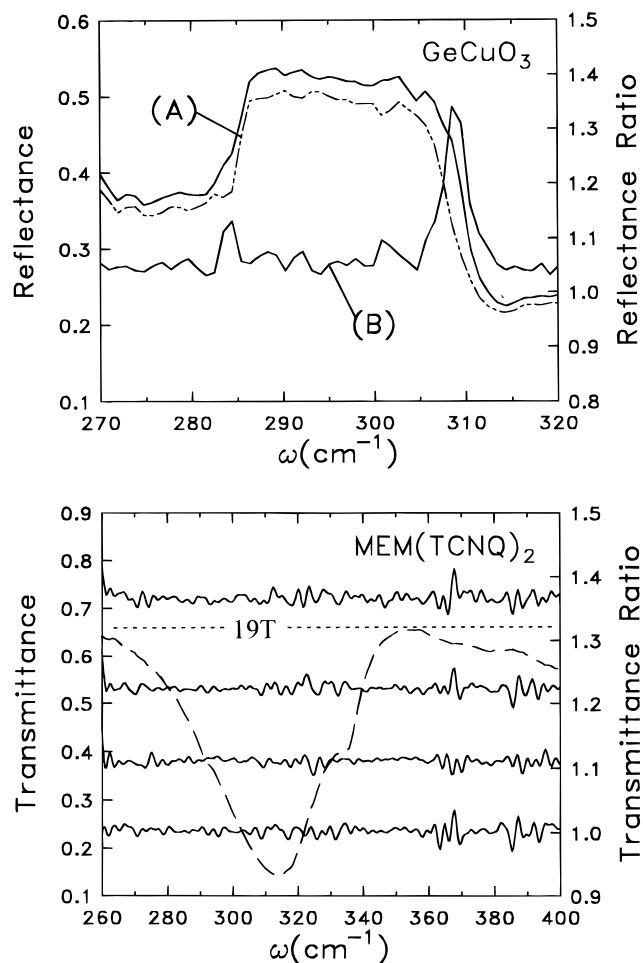The left panel in Figure 2 displays a portion of the power reflectance spectra and the reflectance ratios of

Figure 2. Top panel: (A) 5 K reflectance spectra of $GeCuO_3$ taken at 0, 9, and 17 T. Note that the 0 and 9 T data are indistinguishable here. (B) 5 K reflectance ratios of $GeCuO_3$ as a function of applied field. Solid line, $R(H = 17\ T)/R(H = 0\ T)$; double-dashed line, $R(H = 9\ T)/R(H = 0\ T)$. The 9 T/0 T reflectance ratio provides an estimate of the noise level in these experiments. Bottom panel: dashed line, absolute transmission spectra of $MEM(TCNQ)_2$ at 300 K and zero field; solid lines, 5 K transmission ratios of $MEM(TCNQ)_2$ taken as a function of applied magnetic field. From bottom to top: 5 T/0 T, 10 T/0 T, 15 T/0 T, 25 T/0 T. The ratio curves in both panels have been offset for clarity.

$GeCuO_3$ as a function of magnetic field taken at 5 K.[20] The $H = 0$ T and $H = 9$ T curves were obtained in the SP phase, whereas the $H = 17$ T spectrum was obtained in the high-field magnetic phase. The vibrational mode shown here has been assigned as a B_{3u} shearing mode of the lattice, involving the motion of the CuO_4 squares in the direction of the magnetic chains.[18,19] This mode is sensitive to the SP → I transition, red-shifting upon passing through the phase boundary, due to the nature of the lattice motion in the direction of the spin chain. This change is shown more clearly in the reflectance ratio, which highlights both the red shift of the B_{3u} mode and a slight modification of the leading edge of the band upon entry into the high-field phase. Lorentzian fits of the B_{3u} feature as a function of temperature and field have been successfully used to mimic the reflectance ratio structure shown here.[20,49] Note that within the SP phase, the magnetic field has no effect in this energy

(43) Revcolevschi, A.; Collongues, R. C. *R. Acad. Sci.* **1969**, *266*, 1767.

(44) Almeida, M.; Alcacer, L. *J. Cryst. Growth* **1983**, *62*, 183.

(45) Almeida, M.; Alcacer, L.; Lindegaard-Anderson, A. *J. Cryst. Growth* **1985**, *72*, 567.

(46) The field was applied along the *a* crystallographic axis.

(47) Ng, H. K.; Wang, Y. J. Proceedings of the Physical Phenomena at High Magnetic Fields II Conference, Tallahassee, FL, Fisk, Z., Ed.; 1995.

(48) Li, G.; Dissertation, State University of New York at Binghamton, 1997.
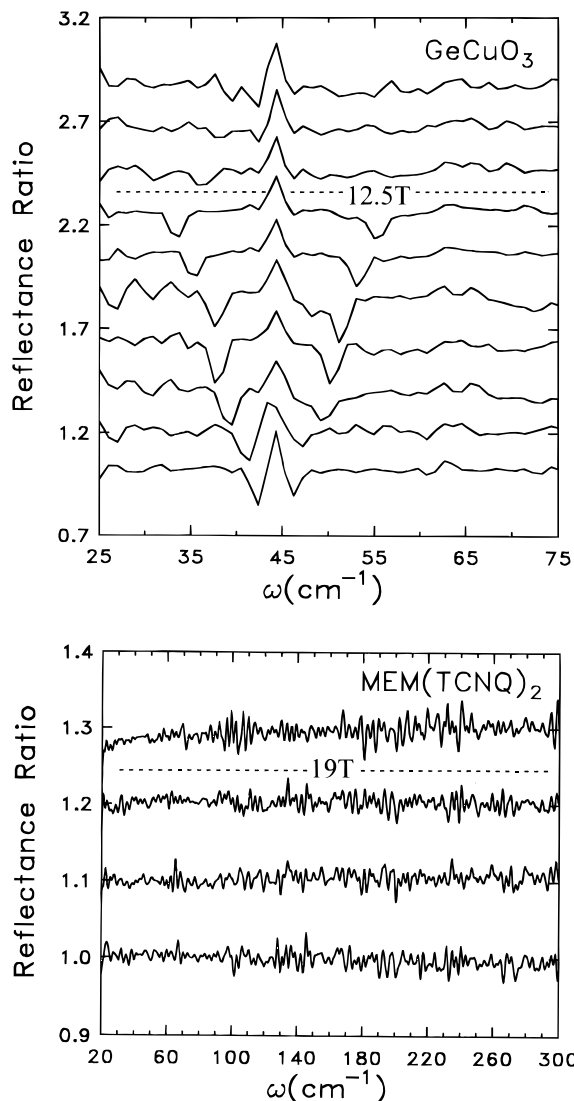
Figure 3. Top panel: reflectance ratios of GeCuO$_3$ in the far-infrared that characterize the dimerized → incommensurate phase transition at 5 K. From bottom to top: 2 T/0 T, 5 T/0 T, 7 T/0T, 9 T/0 T, 11 T/0 T, 13 T/0 T, 15 T/0 T, and 17 T/0 T. The curves have been offset for clarity. Bottom panel: far-infrared transmission ratios of MEM(TCNQ)$_2$ as a function of applied magnetic field at 5 K. From the bottom to the top: 5 T/0 T, 10 T/0 T, 15 T/0 T, and 25 T/0 T. The curves have been offset for clarity.

range, and the reflectance ratio 9 T/0 T is flat and featureless.

In the very far-infrared, the reflectance ratio on the inorganic SP prototype GeCuO$_3$ displays evidence of the zone−center SP gap (left panel, Figure 3.[20,50,51] It is characterized by Zeeman splitting around the 44 cm^{-1} zero-field value of the SP gap, which is a typical result for the field dependence of a triplet state. The leading and trailing dips of this structure disappear upon entry into the high-field incommensurate phase, indicating that the magnetic state is quite different above 12.5 T.

The behavior of the unusual structure observed in the low−energy ratio spectra can be explained by the
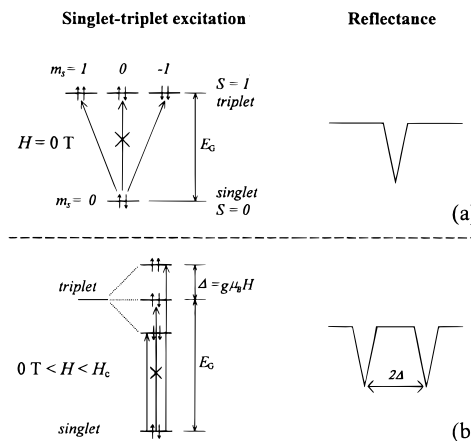
(49) Wooten, F. *Optical Properties of Solids*; Academic Press: New York, 1972.
(50) van Loodrecht, P. H. M.; Huant, S.; Martinez, G.; Dhalenne, G.; Revcolevschi, A. *Phys. Rev. Lett.* **1996**, *76*, 331.
(51) The zone−center gap for GeCuO$_3$ is at 17 cm^{-1}.[11,12]

Figure 4. Magnetic excitations and theoretical reflectance spectra within the low-temperature phase of GeCuO$_3$ (A) at zero field and (B) with applied magnetic field.

Zeeman splitting of the triplet state. Figure 4 sketches the singlet−triplet gap excitation of GeCuO$_3$ within the SP phase and their reflectance spectra in the ideal situation, assuming that the reference reflectance is perfectly flat. At zero field, the $\Delta m_s = \pm 1$ excitations across the SP gap are degenerate, giving rising to a single dip in reflectance at the energy of the SP gap; when applying magnetic field, the triplet state splits, giving rise to two linearly progressing dips in reflectance. Ratioing these two reflectances leads to the unusual structure shown in the reflectance ratio spectrum in Figure 3. After the SP → I transition, the nonmagnetic singlet ground state is destroyed. Without the presence of a singlet−triplet gap, the reflectance becomes flat and the ratio of the reflectance spectrum after SP → I transition to the 0 T spectrum results in a single peak in the ratio spectrum as shown in Figure 3. On the basis of the above discussion, we can clarify that the center peak in the ratio spectrum is related to the SP gap at zero field, while the two moving dips are caused by the Zeeman splitting of the triplet state and the disappearance of these two dips is caused by the SP → I phase transition.

The behavior of the GeCuO$_3$ is contrasted by that of the organic molecular conductor MEM(TCNQ)$_2$, which displays a featureless transmission ratio spectra throughout similar frequency ranges (right panels of Figures 2 and 3). It is well-known that above 150 cm^{-1}, MEM-(TCNQ)$_2$ has a number of IR-allowed intramolecular vibrational modes of B$_{1u}$, B$_{2u}$, and B$_{3u}$ symmetry.[52,53] In addition, the 10 A$_g$ vibrational modes of the TCNQ building block molecule are activated by the electron−phonon (or electron−molecular vibration) coupling process, in which a normally IR silent mode couples with a low-lying electronic charge-transfer excitation.[52,53] These A$_g$ coupling-allowed features appear with enhanced oscillator strength and strong chain−axis polariztion, making them especially sensitive and well-established probes of phase transition processes in TCNQ-based materials. For the energy range shown in the right panel of Figure 2, the spectrum of MEM-(TCNQ)$_2$ contains information on one of the A$_g$ electron−

(52) Rice, M. J.; Yartsev, V. M.; Jacobsen, C. S. *Phys. Rev. B.* **1980**, *21*, 3437.
(53) Yartsev, V. M.; Jacobsen, C. S. *Phys. Rev. B.* **1981**, *24*, 6167.

Spin-Peierls Materials in a Magnetic Field

Chem. Mater., Vol. 10, No. 4, 1998   **1119**

phonon activated modes (ν_9 at 320 cm^{-1}). While evidence of this feature is clear in the single-beam spectra, the transmission ratios show that there is no change in this structure with applied magnetic field. Further, our measurements show that, within our noise level (2−3%), none of the intramolecular modes of the MEM(TCNQ)$_2$ are modified on passing through the SP → I phase boundary. Therefore, we can conclude that neither the normally IR-allowed nor the electron−phonon-activated intramolecular vibrational modes are sensitive to the phase boundary at 19.5 T or the change in magnetic structure accompanying the phase transition. Due to the microscopic nature of the electron−phonon coupling mechanism, we can also rule out any change in the tetrameric structure of the TCNQ chain or the character of the electronic charge-transfer properties upon entry into the high-field incommensurate phase.

Both translational and librational modes, which characterize the long-range vibrational motions of the MEM(TCNQ)$_2$ sample, resonate at low energy (below 150 cm^{-1}).[31,54−58] Although weaker in strength than the aforementioned intramolecular vibrational modes, evidence for several intermolecular modes is also clearly observed in the single beam far-infrared spectrum. However, there are no changes in these structures with applied magnetic field. Therefore, the transmission ratios are flat and featureless within the SP phase and also through the SP → I phase boundary, as shown in the right panel of Figure 3. Thus, we conclude that the intermolecular modes in the frequency range of our investigation (down to 20 cm^{-1}) are not sensitive to the phase boundary.[59]

Although our measurements become fairly noisy near 20 cm^{-1}, we find no clear evidence for the spin-Peierls gap in MEM(TCNQ)$_2$, a structure which might be expected near 22 cm^{-1} since $\Delta = 1.75kT_{sp}^2$. We also did not observe a higher energy SP gap in our measurements, unlike the separate zone−boundary and zone−center gaps in the inorganic prototype discussed above.[11]

Both the lattice structure and the spin localization are important in determining the nature of the magnetoelastic coupling in SP materials, and it is likely that these two effects are responsible for the striking differences observed in the far-infrared spectra of GeCuO$_3$ and MEM(TCNQ)$_2$ reported here. Briefly, the inorganic prototype has an extended linear chain lattice, whereas the organic molecular material is held together only by van der Waals forces. Our measurements suggest that the energy scale of the phonons sensitive to the D → I phase transition are quite different, with lower energy excitations being more important in the organics due to the softer lattice.

The magnetoelastic coupling is also affected by the extent of the spin localization. As previously discussed, the spin system in the organic material is more diffuse, due to the π-type origin of the spins, and delocalized over the TCNQ dimer, than that in the inorganic compound, which has highly localized d-type spins on the Cu sites. Thus, it is reasonable to expect and it is consistent with our observations that the magnetoelastic coupling is overall weaker and of lower energy in the organic solid compared to the linear chain oxide.

4. Conclusion

We have reported far-infrared reflectance and transmission measurements on high-quality samples of GeCuO$_3$ and MEM(TCNQ)$_2$ as a function of magnetic field in order to characterize the microscopic nature of the SP and high-field incommensurate phases in the $H-T$ diagram. For the linear chain inorganic compound, GeCuO$_3$, the far-infrared spectra is incredibly rich, with a B$_{3u}$ shearing mode of the lattice as well as the zone−boundary SP gap sensitive to the high-field boundary in the $H-T$ phase. In contrast, the traditional organic molecular conductor MEM(TCNQ)$_2$ shows no changes in either the intramolecular or intermolecular modes above 20 cm^{-1} at the high-field boundary. This difference is discussed in terms of the spin localization and the extended vs molecular structure of the two solids.

(54) Tanaka, Y.; Satoh, N.; Nagasaka, K. *Synth. Met.* **1991**, *41−43*, 2503.

(55) Tanaka, Y.; Nagasaka, N. *Solid State Commun.* **1990**, *73*, 735.

(56) Oostra, S.; De Lange, P.; Visser, R. J. J. *J. Phys., Col. 3* **1983**, *44* (6), C3−1383.

(57) Ohta, H.; Homma, K.; Nagasaka, K. *J. Phys. Soc. Jpn.* **1985**, *54*, 4390.

(58) This separation between intramolecular (above 150 cm^{-1}) and intermolecular modes (below 150 cm^{-1}) is somewhat artificial but useful and is based on the structure of the organic building block unit. The intramolecular modes of the molecular can be obtained from a normal coordinate analysis, whereas the intermolecular modes of the organic molecular solid reflect the extended nature of the material.

(59) In the future, it is important to extend these experiments to lower energy to follow any changes in the 8 cm^{-1} soft mode with field.[31] However, the limited frequency range of our apparatus precludes us from doing these experiments ourselves.